

# Thrust Measurement of Deployable Propeller for Powered Paraglider in Mars Atmosphere

K. Hiraki<sup>1</sup>, S. Tashima<sup>1</sup> and M. Namikawa<sup>1</sup>

<sup>1</sup>Department of Mechanical and Control Engineering  
 Kyushu Institute of Technology, Kitakyushu, Fukuoka 804-8550, Japan

## Abstract

A preliminary design of a propeller of the powered paraglider for Mars exploration was conducted. The blade design was made with the computational method developed by Adkins and Liebeck. In order to obtain the necessary thrust of 7.88N, the propeller diameter was computed to 1.0m. Thus, the propeller should be retracted in an entry probe, and it should have self-deploying capability. A one-fourth scaled model of the propeller was fabricated to demonstrate its capability and thrust. The special thrust-measurement device was designed for a wind-tunnel test. Some disagreement was found in the comparison between the measured and predicted thrust. In order to clarify the reason of the discrepancy the aerodynamic data of the wing in low Reynolds number environment were obtained in the wind tunnel. Based on the data obtained the thrust prediction was redone. The agreement was improved and it validated the design process of the blade in this study.

## Introduction

In the past years a number of spacecraft have been sent to Mars: The Mars orbiters mapped the whole surface of the planet and obtained images with good resolution, and the ground rovers were also successful to carry out the in-situ scientific analyses in detail. These rovers can move to the desired area under their own power, however, the travelling speed is quite low. In order to enlarge the field of the investigation with limited resources it is advantageous to employ an aerial vehicle.

However, the design of such an aerial vehicle in Martian atmosphere should be more difficult than that on Earth, because the properties in Martian atmosphere are quite different to those on Earth. In Table 1 comparisons were made on the environments at the surface on Mars and Earth, regarding not only the atmospheric properties but also the accelerations of gravity.

Since the atmospheric density is thin on Mars, the flight speed of such a vehicle must be high enough to sustain its own weight, with a limited wing area. A high speed flight could give undesired influence on the scientific measurement. In order to avoid this problem the aerial vehicle using a paraglider is proposed [1]. This aerial vehicle has two big advantages. First, the flight speed could be drastically reduced because of its deployable large wing area. Secondly, it can be controlled by a simple mechanism and can land softly at a desired spot on the Martian surface.

	Mars	Earth
Acceleration of Gravity [m/s <sup>2</sup> ]	3.71	9.81
Atmospheric Pressure [kPa]	0.7	101.3
Atmospheric Density [kg/m <sup>3</sup> ]	0.02	1.23
Viscosity*10 <sup>-5</sup> [Pa s]	1.06	1.82
Speed of Sound [m/s]	230	340

Table 1. Comparisons of environments at surface in Mars and Earth.

In order to gain the exploration time of two hours the aerial vehicle employing a paraglider should equip some propulsive device which could overcome the aerodynamic drag on the vehicle. The most conventional way to generate thrust is a rotating propeller. In Fig.1 the Martian flight of the aerial vehicle with the powered paraglider is schematically presented.

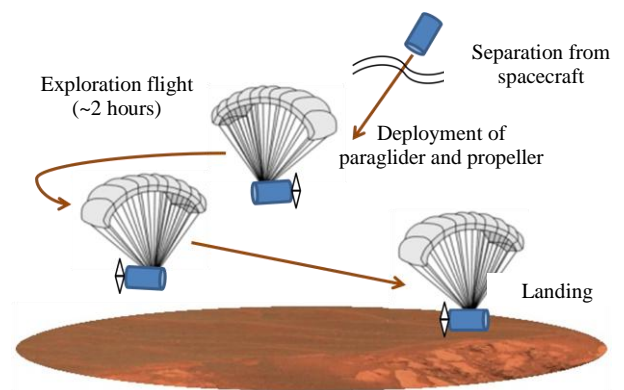


Figure 1. Schematics of powered-paraglider in Martian atmosphere.

## Design of Propeller Blade

From the result of the sizing of an aerial vehicle, a paraglider for Mars exploration was proposed with the following specifications listed in Table 2 [2]. Based on the specifications mentioned above, the requirements on the propulsive device were calculated. The necessary thrust was calculated to 7.88N. From the viewpoint of the mass budget for a two-hour long flight, the upper limit of input power was set to 500W.

Wing area [m <sup>2</sup> ]	22.7
Aspect ratio	3.0
Cruising speed [m/s]	27.7
Lift coefficient at cruise	0.50
Lift-to-drag ratio	6.99

Table 2. Assumed specification of paraglider for Mars exploration.

The preliminary design of the propeller blade was made using the computational method which was developed by Adkins and Liebeck [3]. This method treats not only the flow around the blade elements but also the wake flow with a spiral structure behind the propeller. It gives the optimum blade shape with maximum efficiency when the flight speed, the number of the blade, the radius and rotational speed of the propeller, and the sectional shape and design attack angle of the blade are given.

### Propeller Radius

First of all, the number of blades was set to two for mass reduction. Figure 2 shows the revolution number of the propeller for each propeller radius when the tip of the blade reaches to the sonic condition in Martian atmosphere. If the propeller radius is around 0.5 m, the revolution number should be below 4,000 rpm in order to avoid compressibility effects of the atmosphere.

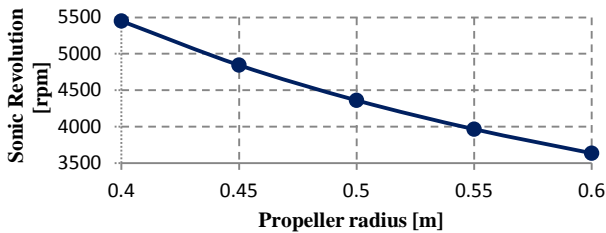


Figure 2. Revolution number at sonic condition for each propeller radius.

Three kinds of wing section shape were selected as a candidate, DAE51, SD7037 and Clark-Y with nine percent thickness. All of them are known to have good performance especially in low Reynolds number condition. Figure 3 compares the input power to generate the necessary thrust for the three different blade-section shapes. In the present analysis the propeller inner radius was set to ten percent of that the propeller and the design angle of attack was set to five degrees. Since the upper limit of the input power was 500W, the radius of the propeller should be larger than 0.45m. Furthermore, the input power tends to increase after the radius becomes beyond 0.55m. Thus, the propeller radius was determined to 0.5m for the further analysis.

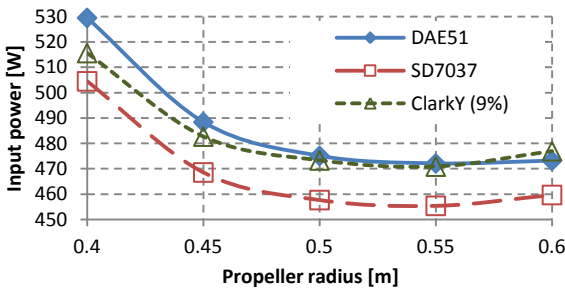


Figure 3. Input power for various propeller radii with different wing section.

Now, the diameter of the propeller is 1.0m, whereas the envelope of the vehicle inside an entry probe was assumed 0.5m at maximum. Therefore, the propeller must be retracted in some way to be stored in the probe. Figure 4 shows a conceptual schematic for retraction of the propeller. In this configuration the root side of the blade cannot be used for the thrust generation, and, then the inner diameter of the propeller should be 0.5m for the further analysis.

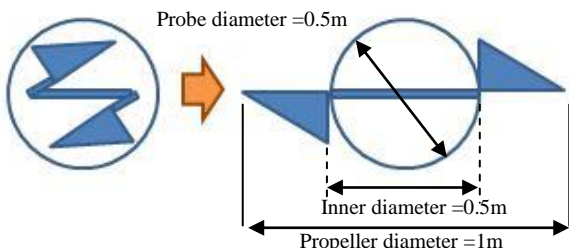


Figure 4. Retraction of propeller and the definition of inner diameter.

### Sectional Shape and Design Angles of Attack

Based on the conditions described previously, the input power was calculated for the three different sectional shapes, varying the design angles of attack, as shown in Figure 5. As was mentioned previously, the maximum input power was limited to below 500W. DAE51 was not affordable when the design angles of attack were over five degrees. For SD7037 and Clark-Y, the input power was acceptable in the range of the design angles of attack shown here.

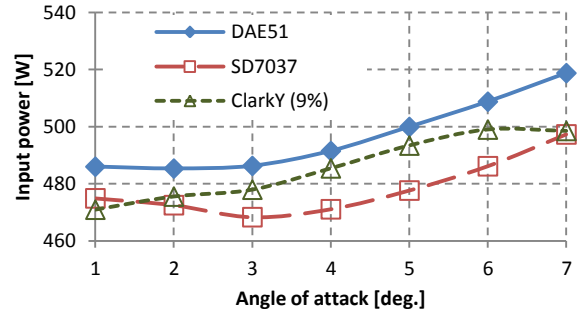


Figure 5. Relation between input power and the design angle of attack.

Figure 6 displays the maximum chord length of the blade for the three different sectional shapes, varying the design angles of attack. It is clear that the blade needs the larger chord length when the design angles of attack are small. Considering the retraction of the propeller, the maximum chord length should be limited under 0.3m. Then, the design angles of attack should be greater than six degrees. Based on these discussions, the design angles of attack of the blade was set six degrees, and SD7037 was chosen as the sectional shape, because it required the lowest input power at six degrees of attack angle, as shown in Figure 5.

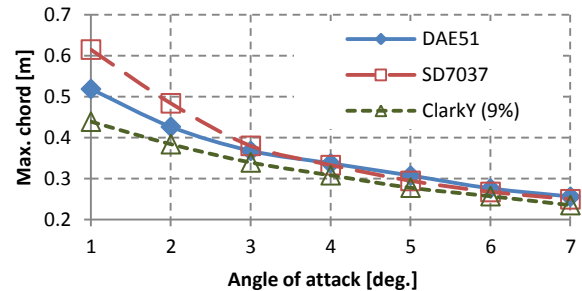


Figure 6. Relation between maximum chord and design angle of attack.

Finally, the optimum blade shapes can be obtained. Figure 7 shows the final result of the blade in terms of the chord-length and twist-angle distribution along the blade radius.

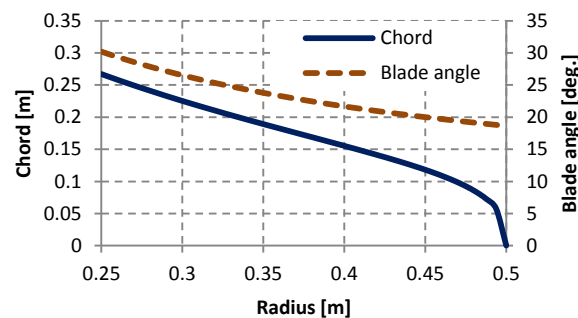


Figure 7. Chord length and twist angle of blade as a function of blade radius.

### Retractable Propeller

Figure 8 illustrated the deployment sequences of the retracted propeller. At first, the propeller was stored inside of the entry probe of which cross section was colored in orange. When the retracted propeller starts the rotation, the centrifugal force acting on the blade promotes the deployment. As was shown in the figure, the blade can rotate around the single axis, and its rotation was limited by the stopper pin, which firmly held the blade when the propeller was fully deployed.

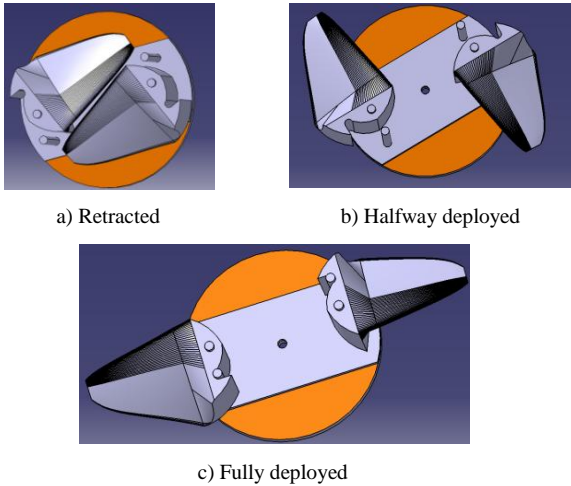


Figure 8. Deployment sequences of retracted propeller.

### Deployment Test of Scaled Model

In order to validate the self-deployment capability of the retractable propeller, the one-fourth scaled model was fabricated. It was driven by an electrical motor, and the deployment process was observed. It successfully demonstrated its self-deployment capability. The pictures taken during the deployment experiment were presented in Figure 9.

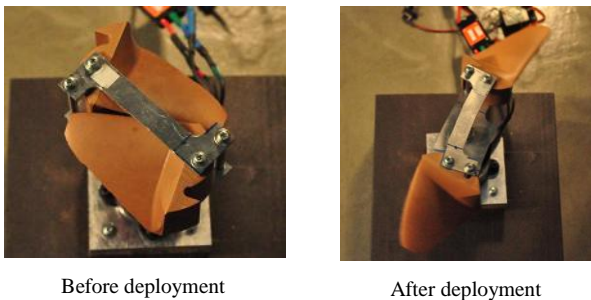


Figure 9. Deployment experiment of scaled model of retractable propeller.

### Thrust Measurement in Wind Tunnel

#### Thrust Measurement Device

The thrust measurement was conducted in the low-speed wind tunnel using the one fourth scaled propeller model. Since the lowest thrust was expected in the order of 1N, the device had to be made for this purpose. Figure 10 shows the schematic of the thrust-measurement device. In this device the propeller with a motor was attached at the tip of the linear rail. This rail was connected through a spring to the base. When the propeller generates thrust force, it elongates the spring. Thus, the displacement of the linear rail should be measured instead of the direct force. It can be measured precisely by the aid of a laser displacement sensor. In order to balance the linear rail in the right

position the linear rail was preloaded by the weight through the wire. This preload eliminates the effect of the static frictional force of the rail. This device was calibrated in the range from 0.7N to 7N. The advantage of this technique is to eliminate the vibration which is caused by the rotation of a motor. It allows one to measure the thrust more precisely. This technique is applicable in various force range by selecting appropriate spring. This is another advantage of this technique.

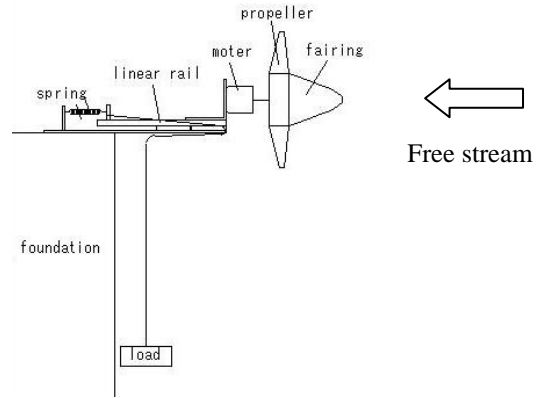


Figure 10. Thrust measurement device.

Using the apparatus described above, the thrust measurement of the scaled propeller was measured by varying the rotational numbers. The wind speed was 6.4m/s. With this free-stream speed the angles of attack of the blade estimated from four to six degrees. The Reynolds number was also estimated from 26,000 to 127,000.

The measured values of the propeller thrust were plotted as a function of the rotational numbers in Figure 11. In the figure the predicted values were also presented which were obtained according to the Adkins and Liebeck's method in the wind-tunnel condition. The agreement between the predicted and measured values were not so bad, however, the discrepancy becomes apparent when the rotational number increased above 3,300 rpm.

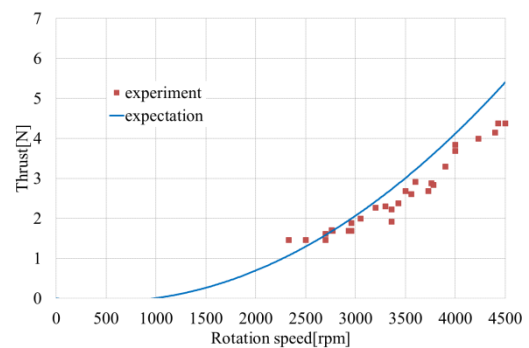


Figure 11. Comparison of thrust between measurement and prediction.

### Aerodynamic Characteristics of Wing

The reason of the discrepancy was not clear. In the computing process of the blade the estimated aerodynamic data for the wing section SD7034 were used. Especially, in the low Reynolds number regions such aerodynamic properties are not sufficiently available. Thus, the aerodynamic data for SD7037 were estimated by the two-dimensional viscid analysis. This might be a source for the errors which were shown in Figure 11. Therefore,

the wind-tunnel test was planned to evaluate the aerodynamic data.

Figure 12 depicted the experimental setups for the two-dimensional wing in the wind tunnel. Since the test section was open to the air, the side walls were installed at both ends of the wing model. The aerodynamic forces were measured by the sensors located beneath the test section. The wind speed was 10m/s, which corresponded to the Reynolds number of 60,000, based on the chord length.

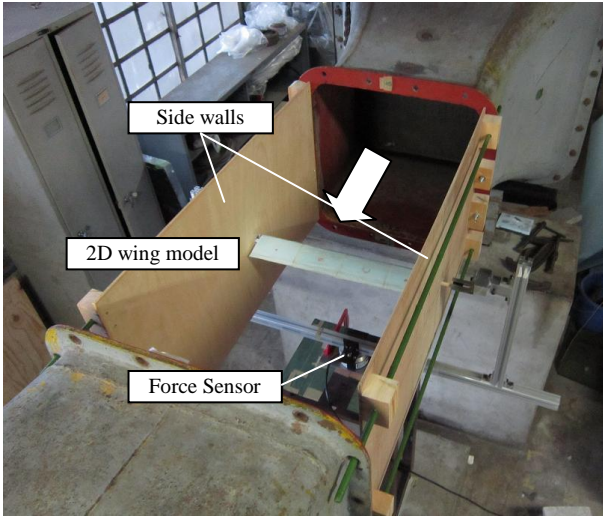


Figure 12. Wind-tunnel test setup for 2D wing model.

The measured lift and drag curves were shown as a function of angles of attack in Figure 13. The solid and open circles indicate the measured values. The analytically estimated values were also presented in the figure, in the form of solid and open boxes. In the lift curves the measured value had larger values at the angles of attack of three degrees. However, the aerodynamic data in the small angles of attack were not used in the design process of the blade. The most effective range of the angles of attack on the thrust was from four to six degrees. In such a range the estimated lift values were greater than the measure values. In the range of the rotational number of the propeller where the discrepancy of the thrust was apparent, the Reynolds numbers were greater than 50,000. This meant that in the computing process the thrust was overestimated due to the higher lift curves.

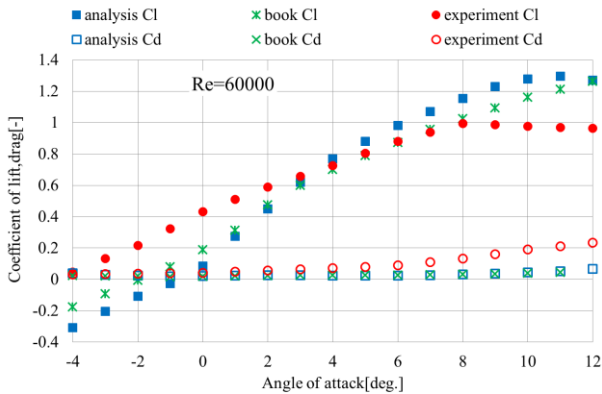


Figure 13. Comparisons of lift and drag coefficients for SD7037 at Reynolds number of 60,000.

### Re-Evaluation of Thrust

Based on the discussions described so far, the prediction of the thrust was redone, using the measured aerodynamic characteristics of SD7037 wing section. The results were compared to the measured thrust in Figure 14. The agreement was better than that in the previous figure. This indicates that the design process presented in the study is valid as long as the appropriate aerodynamic database was available. Thus, the design work for the Mars powered paraglider could be continued with the present tools.

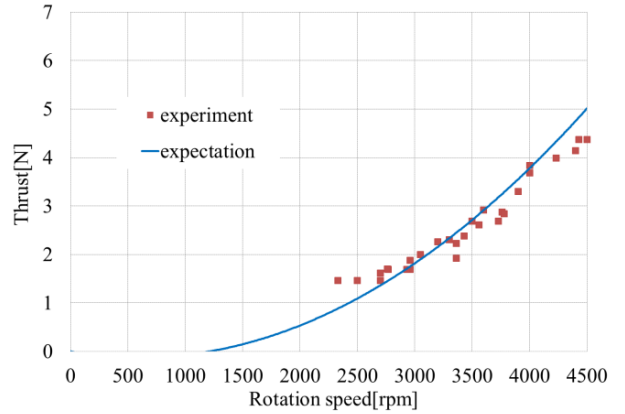


Figure 14. Comparisons of the measured and the re-predicted thrust.

### Conclusions

A preliminary design of a propeller of the powered paraglider for Mars exploration was conducted. The blade design was made with the computational method developed by Adkins and Liebeck. In order to obtain the necessary thrust of 7.88N, the propeller diameter was required to be 1.0 m. The propeller was designed for retraction inside an entry probe, and must have the self-deploying capability. A one-fourth scaled model of the propeller was fabricated to demonstrate its capability and thrust. In the deployment experiment it showed successfully its self-deployment capability. A special thrust measurement device was designed for a wind-tunnel test. Some disagreement was found in the comparison between the measured and predicted thrust especially in the higher rotational numbers. In order to clarify the reason of the discrepancy, the aerodynamic data of the two-dimensional wing in a low Reynolds number environment were obtained in the wind tunnel. Based on the data obtained the thrust prediction was redone. The agreement was improved, and it validated the design process of the blade in this study.

### References

- [1] Hiraki, K., Hidaka, Y., Abe, T., Yamada, K., Higashino, S., Aerodynamic Advantages of Compulsively-Inflated Paraglider for Mars Exploration, Eighth International Conference on Flow Dynamics (ICFD), Sendai, 2011, Nov.9-11.
- [2] Hiraki, K., Hidaka, Y., Improvement of Lift-to-Drag Ratio of a Parafoil for Mars Exploration, 28<sup>th</sup> International Symposium on Space Technology and Science, ISTS2011-e-13, 2011.
- [3] Adkins, C. N., Liebeck, R. H., Design of optimum propellers, Journal of Propulsion and Power, vol. 10 (1994), no. 5, pp 676-682.